Langmuir

Article

pubs.acs.org/Langmuir

How Does the Ethoxylated Grafting of Polyelectrolytes Affect the Self-Assembly of Polyanion–Cationic Surfactant Complex Salts?

Ana Maria Percebom,[†] Leandro Ramos Souza Barbosa,[‡] Rosangela Itri,[‡] and Watson Loh*[,†]

[†]Institute of Chemistry, University of Campinas (UNICAMP), CP 6154 Campinas, SP Brazil

[‡]Institute of Physics, University of São Paulo (USP), CP 66318 São Paulo, SP Brazil

Supporting Information

ABSTRACT: A cationic surfactant and different anionic copolymers randomly grafted with side chains of ethylene oxide were used to prepare stoichiometric complex salts. Variations in the length or proportion of side chains were shown to be responsible for affecting the surfactant phase behavior in water, resulting in the observation of a number of structures characterized by small angle X-ray scattering measurements, including a hierarchical micellar system and different liquid-crystalline phases. Additionally, although aqueous mixtures of stoichiometric complex salts usually phase separate, the presence of a sufficiently high weight fraction of ethylene oxide side chains can enhance the solubility of the complex salt aggregates in water over a wide range of concentration. Moreover, a dispersion of an isotropic concentrated solution of complex salts is formed at higher temperatures in a reversible process. In summary, this study proves the importance of the polyion structure for tuning the properties of systems of complex salts.

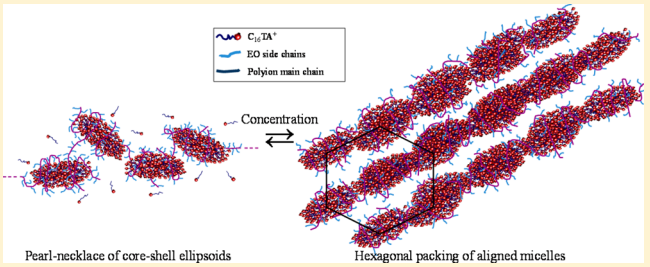

1. INTRODUCTION

It is well known that polymers can affect the self-assembly of surfactants by modifying their phase behavior. In particular, the systems formed by oppositely charged polyelectrolytes and ionic surfactants are of growing interest because of the occurrence of an associative phase separation. The strong electrostatic attraction between the two species leads surfactants and polymers to associate, forming the so-called complex salt, which may separate out under certain conditions, in a concentrated phase with different possible structures (disordered micellar or liquid-crystalline phases).[1,2] The formation of this concentrated phase has attracted attention to complex salts because of the possibility of applications as gelling agents,[3] for drug delivery,[4] in personal care products,[5] for DNA compaction,[6] and even for tailored nanostructured materials.[7]

For all purposes, knowledge of the effects of the chemical structure on the properties of complex salts is necessary to achieve systems with the needed features. This fact highlights the importance of systematic studies of the phase behavior and structural characterization of complex salts formed by different polymers and surfactants. Recent studies have investigated complex salts formed by tetraalkylammonium surfactants and acrylate/methacrylate-based polymers by evaluating the effects of changing the surfactant chain length or the polyion length, as described in recent reviews.[8,9] However, not much attention has been paid to the role of different architectures of polyions in the phase behavior of complex salts. Most studies involving block or grafted copolymers are concerned only with the characterization of the aggregates formed in dilute aqueous systems at different surfactant/polymer ratios.[10−14]

On the basis of that, the aim of this study is to investigate the effect caused by grafting ethylene oxide oligomers onto a methacrylate-based polyion on the phase behavior and self-assembly of a cationic surfactant and to characterize the structures formed in aqueous mixtures with concentrations of up to 80 wt % of the complex salt. One could expect the formation of aggregates of the complex salt solubilized in water because of the presence of hydrophilic oligomers of ethylene oxide. Indeed, we have used the strategy of grafting to obtain water-soluble complex salts, which were demonstrated to form equilibrium aggregates by a cooperative process, as better described in a recent publication.[15] Here, we collate systems of complex salts with different fractions of grafted monomers or with side chains of different lengths and also contrast these with the previously investigated complex salt of the analogous homopolyion (polymethacrylate).

To highlight the effect of the copolymer and for an easier examination of the phase behavior, a strategy developed by Svensson et al. is used to remove the simple counterions and to prepare pure complex salts with a stoichiometric charge ratio.[16] Small-angle X-ray scattering (SAXS) is used for the characterization of the different formed structures and allowed us to identify a rich phase behavior. Disordered (micellar) phases are analyzed by fitting a combination of an effective ellipsoidal

Received: May 26, 2014
Revised: August 27, 2014
Published: September 10, 2014

core−shell and a pearl-necklace models to the scattering of micellelike aggregates, and liquid-crystalline phases are analyzed by their characteristic Bragg reflections. Because of the presence of ethylene oxide chains, which exhibit lower critical solution temperature behavior in water, thermal effects are investigated by analyses at different temperatures and by high-sensitivity differential scanning calorimetry measurements.

2. METHODS AND EXPERIMENTAL SECTION

The studied complex salts were prepared with C_{16}TAOH (hexadecyltrimethylammonium hydroxide) and the random copolymers poly(methacrylic acid-*co*-methacrylate ethoxylated), P(MAA-MAEO$_n$) *x*:*y*, where *n* is the number of ethylene oxide units in each side chain and *x*:*y* is the molar proportion of MA/MAEO$_n$. These copolymers are P(MAA-MAEO$_5$) 72:28, P(MAA-MAEO$_5$) 36:64, and P(MAA-MAEO$_{24}$) 69:31 with weight-average molar masses of 1.62×10^5, 1.99×10^5, and 1.43×10^5 Da and polydispersities of 2.7, 3.8, and 1.6, respectively. A complete description of the materials and methods for the synthesis and characterization of copolymers, the preparation of complex salts, and phase diagram determination can be found in the Supporting Information.

2.1. Small Angle X-ray Scattering Experiments. SAXS measurements were performed at the SAXS1 and SAXS2 beamlines of the Brazilian Synchrotron Laboratory (LNLS) in Campinas, Brazil. Samples were positioned in a cell with a mica or Kapton window under water-bath temperature control. The distance between the sample holder and detector varied between 500 and 1600 mm, and the X-ray wavelength was λ = 1.488, 1.550, or 1.608 Å. Fit2D[17] software was used to integrate CCD images and to subtract parasitic background and solvent scattering (blank) whenever necessary, and GENFIT software[18,19] was used for the fitting procedure.

2.2. Cloud-Point Measurements. To follow the turbidity changes caused by increasing temperature, absorbance measurements were performed using an HP 8453 UV−visible spectrophotometer at a wavelength of 410 nm and UV-Visible ChemStation software. Each sample in a glass cuvette was control heated at a rate of 1.5 °C/min by an HP 89090A temperature controller in the range of 20 to 80 °C. After reaching the highest temperature, the sample was cooled back to 20 °C. The experiment was then repeated after the temperature was equilibrated. The second curve was always identical to the curve of the first experiment. The data are reported as absorbance as a function of temperature. The cloud points of the samples were obtained at the onset of the experimental curves. The analyzed samples were dilute aqueous solutions of either copolymers or complex salts with concentrations of between 0.4 and 0.6 wt %.

2.3. Differential Scanning Calorimetry. To investigate possible transitions induced by increasing temperature, the same samples analyzed by spectrophotometry (aqueous solutions of either copolymers or complex salts with concentrations between 0.4 and 0.6 wt %) were analyzed using a VP-DSC (MicroCal, Northampton, MA) calorimeter in the range of 20−80 °C and at scanning rate of 1.5 °C/min. This equipment uses two 0.54 mL total-filled cells: one for the sample solution and another one for water as a reference cell. The samples were equilibrated for 10 min before each scan. Each experiment was conducted in triplicate, and the first scan was neglected. The baseline reference, obtained by conducting an experiment with both cells containing water, was subtracted from the sample thermograms. For instrument control, acquisition, and data analyses, MicroCal Origin 5.0 and OriginPro 8 software were used.

3. RESULTS AND DISCUSSION

3.1. Effects of Polymer Structure on the Phase Behavior of Complex Salts. For the determination of three binary phase diagrams of complex salts in water at 25 °C (Figure 1), a total of 50 samples with different compositions were prepared. On the basis of visual inspection, 26 were selected to be analyzed by SAXS. (The compositions of all samples prepared and analyzed in the phase behavior study of the three complex salts are provided as Supporting Information.) All of the samples formed by C_{16}TAP(MA-MAEO$_5$) 36:64 are isotropic and display viscosity increasing with concentration. SAXS curves confirm that the systems are in the aqueous disordered phase for up to 80 wt % complex salt, as follows. For the system of C_{16}TAP(MA-MAEO$_{24}$) 69:31, samples with concentrations of up to 62 wt % are isotropic and present viscosity increasing with concentration. In particular, samples with concentrations of between 50 and 62 wt % present shear birefringence and viscoelastic behavior, suggesting the formation of highly anisometric aggregates. Samples with concentrations of up to 54 wt % C_{16}TAP(MA-MAEO$_5$) 72:28 display two well-defined phases: a dilute one consisting essentially of pure water and a concentrated bottom one that contains the complex salt and water forming a birefringent liquid-crystalline phase. At higher concentrations, the liquid-crystalline phase persists but its structure evolves as discussed later.

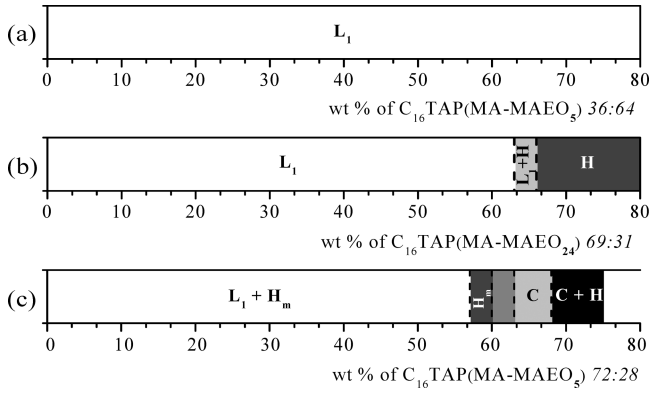

Figure 1. Binary phase diagrams at 25 °C in water expressed in wt % of the following complex salts: (a) C_{16}TAP(MA-MAEO$_5$) 36:64, (b) C_{16}TAP(MA-MAEO$_{24}$) 69:31, (c) C_{16}TAP(MA-MAEO$_5$) 72:28. L_1, Disordered aqueous phase; H_m, hexagonal close-packing of spheres; C, cubic *Pm*3*n*; H, hexagonal packing of cylinders.

At room temperature, C_{16}TAP(MA-MAEO$_5$) 36:64 and C_{16}TAP(MA-MAEO$_{24}$) 69:31 are highly soluble in water: aqueous mixtures of these complex salts display only a single disordered phase (L_1) over a wide range of concentration. The micellization process and the chemical nature of the aggregates formed in dilute solutions of C_{16}TAP(MA-MAEO$_5$) 36:64 and C_{16}TAP(MA-MAEO$_{24}$) 69:31 have been investigated and described in a recent study.[15] However, the aggregates of C_{16}TAP(MA-MAEO$_{24}$) 69:31 eventually form a liquid-crystalline phase with increasing concentration. Despite the fact that C_{16}TAP(MA-MAEO$_5$) 36:64 and C_{16}TAP(MA-MAEO$_{24}$) 69:31 possess similar weight fractions of EO groups (42 and 53 wt % of EO, respectively, as shown in Table S1, see Supporting Information), the aggregates of the first do not form liquid-crystalline phases even at complex salt concentrations as high as 80 wt %, as shown in Figure 1a. The major difference between the two complex salts is the length of their EO side chains: C_{16}TAP(MA-MAEO$_5$) 36:64 possesses shorter and more numerous side chains for similar wt % of EO when compared to C_{16}TAP(MA-MAEO$_{24}$) 69:31. As a consequence, C_{16}TAP(MA-MAEO$_5$) 36:64 displays a lower polyion charge density or, in other words, a greater number of methacrylate neutral comonomers in the polyion main chain, forming more and longer loops and tails rich in neutral comonomers than

dx.doi.org/10.1021/la5019604 | Langmuir 2014, 30, 11493−11503

C_{16}TAP(MA-MAEO$_{24}$) 69:31. Because of the random distribution of neutral and charged comonomers in the polyion, we assume that there is a variation in the distance-dependent attractive forces between the micelles owing to the heterogeneity of the polyion chain surrounding the surfactant aggregates. This heterogeneity should prevent the packing of the aggregates in a long-range-ordered structure, such as liquid crystals. A similar argument was earlier used to explain two phenomena in complex salt self-assembly: the precluding of a liquid-crystalline phase in systems of complex salts formed by other random polyions[20] and the transition to a disordered phase due to the replacement of acetate by polyacrylate counterions in a cubic phase of cetyltrimethylammonium acetate.[21]

The phase behavior of complex salts formed by $C_{16}TA^+$ and carboxylate-based counterions (with different degrees of polymerization) free of simple salts has been investigated by Piculell and coworkers. These studies demonstrate that polymeric counterions give rise to strong attraction among the surfactant micelles, condensing them into a concentrated phase.[21−23] In addition, these authors have shown that demixing can be avoided by replacing a molar fraction greater than 90 mol % of ionized monomers by neutral groups.[24] Although the fraction of neutral comonomers is an important factor, the present study indicates that the side chains of ethylene oxide are essential to the complex salts' solubility in water because the goal was achieved with a molar fraction of only 31 mol % neutral comonomers. However, only the presence of oligo(oxyethylene) units is not enough to significantly increase the complex salt solubility in water. The addition of (EO)-based nonionic surfactant affects the phase behavior and the formed structures in systems of DNA-C_{12}TA complexes but does not lead to solubilization in water.[25] The postaddition of penta- and octa(oxyethylene) dodecyl ether surfactants ($C_{12}EO_5$ and $C_{12}EO_8$) to aqueous systems of C_{16}TAPA complexes increases the repulsion between aggregates and can even dissolve the complex salt, but the maximum dissolution is low (<20 wt % of $C_{16}TAPA_{25}$) and is achieved only with the addition of around 30 wt % $C_{12}EO_8$.[26] The picture suggested is that the aggregates formed in the latter case are composed of clusters of mixed micelles (nonionic and cationic) connected by the polyanion chains, but the mixed micelles are not capable of incorporating enough nonionic surfactant to make the complex salt soluble in water.[26] The great advantage of C_{16}TAP(MA-MAEO$_5$) 36:64 and C_{16}TAP(MA-MAEO$_{24}$) 69:31 is that the hydrophilic EO chains are covalently attached to the complex salt, forming only one species and being necessarily part of the formed aggregates. When the EO chains are introduced into the system by the addition of nonionic surfactants, it is not likely that all of the added molecules will be forced into the micelles of complex salts. A similar strategy was used in a previous study of complexes formed by sodium dodecyl sulfate with different random cationic copolymers of methoxy poly(ethylene glycol) monomethacrylate and (3-(methacryloylamino)propyl)-trimethylammonium chloride.[27] However, turbidity measurements indicate that for a content of 68 mol % comonomers with ethoxylated side chains (EO_8), those complexes are insoluble in water, and only for high contents of neutral groups do the complexes form micellar solutions in water: 89 mol % comonomers with EO_8 or higher, corresponding to around 68 wt % EO groups.[27]

The complex salt with fewer and shorter side chains, C_{16}TAP(MA-MAEO$_5$) 72:28, phase separates even at a small concentration of complex salt (<0.49 wt %), as previously observed for most of the stoichiometric mixtures of oppositely charged polyions and surfactants in water, forming a liquid-crystalline phase coexisting with pure water. This is a clear proof that the mass fraction of ethylene oxide groups in the complex salts directly affects the solubility in water because water-soluble complex salts C_{16}TAP(MA-MAEO$_5$) 36:64 and C_{16}TAP(MA-MAEO$_{24}$) 69:31 possess 42 and 53 wt % EO, respectively, while C_{16}TAP(MA-MAEO$_5$) 72:28 contains only 17 wt % EO groups.

Considering a comparable complex salt of homopolymer, $C_{16}TAPMA_{80}$ (a previously studied complex salt of hexadecyltrimethylammonium surfactant with poly(methacrylic acid) with ca. 80 monomers units),[28] the binary phase diagram of C_{16}TAP(MA-MAEO$_5$) 72:28 displays a larger two-phase region (miscibility gap) than the phase diagram for the complex salt with the related homopolymer.[28] The mesophase formed by C_{16}TAP(MA-MAEO$_5$) 72:28 can incorporate only 44 wt % water against 68 wt % that can be incorporated by the mesophase of $C_{16}TAPMA_{80}$. This means that, although the copolymer has EO hydrophilic side chains, it conveys to the complex salt lower miscibility with water than the homopolymer. A comparison of the weight fractions of $C_{16}TA^+$ at the phase boundaries (25 wt % of $C_{16}TA^+$ for C_{16}TAP(MA-MAEO$_5$) 72:28 and 32 wt % for $C_{16}TAPMA_{80}$) of these complex salts confirms this fact. A possible reason for this may be that the hydrophilic side chains replace water molecules at the aggregate solvation shell. Another explanation for that concerns the length of the polyion: P(MAA-MAEO$_5$) 72:28 contains around 329 acid and 128 neutral comonomers units, while the used poly(methacrylic acid) contains only 80 monomers. In a previous study using poly(acrylic acid) with different numbers of monomer units (30 and 6000), it has been demonstrated that the longer the length of the polyion, the lower the miscibility of the complex salt with water.[22] Probably, for short distances, increasing the length of the polyions makes the interaction between the micelles attractive rather than repulsive, due to polyion bridging among surfactant aggregates and to ion correlation effects, limiting the capacity of the complex salt to incorporate water.

Phase diagrams of complex salts C_{16}TAP(MA-MAEO$_5$) 72:28 and C_{16}TAP(MA-MAEO$_{24}$) 69:31 exhibit large regions of coexistence of two concentrated phases: L_1 + H (Figure 1b), H_m + C and C + H (Figure 1c). A possible reason for this feature is that the copolymers display a significant heterogeneity both in molecular weights and chemical compositions, giving rise to different structures that may coexist in equilibrium over a wider concentration range.

A detailed description of the structures formed by the three investigated complex salts in water with different concentrations is provided, as follows.

3.2. C_{16}TAP(MA-MAEO$_5$) 36:64 + Water. It is well known that the scattering intensity ($I(q)$vs q, with $q = (4\pi/\lambda)\sin(2\theta)$ being the modulus of the scattering vector and 2θ being the scattering angle) from particles of small anisometry can be described as[29]

$$I(q) = nP(q)\,S(q) \tag{1}$$

where $P(q)$ corresponds to the orientationally averaged form factor and $S(q)$ is the interparticle structure factor, which takes into account the interaction between adjacent scattering

dx.doi.org/10.1021/la5019604 | Langmuir 2014, 30, 11493−11503

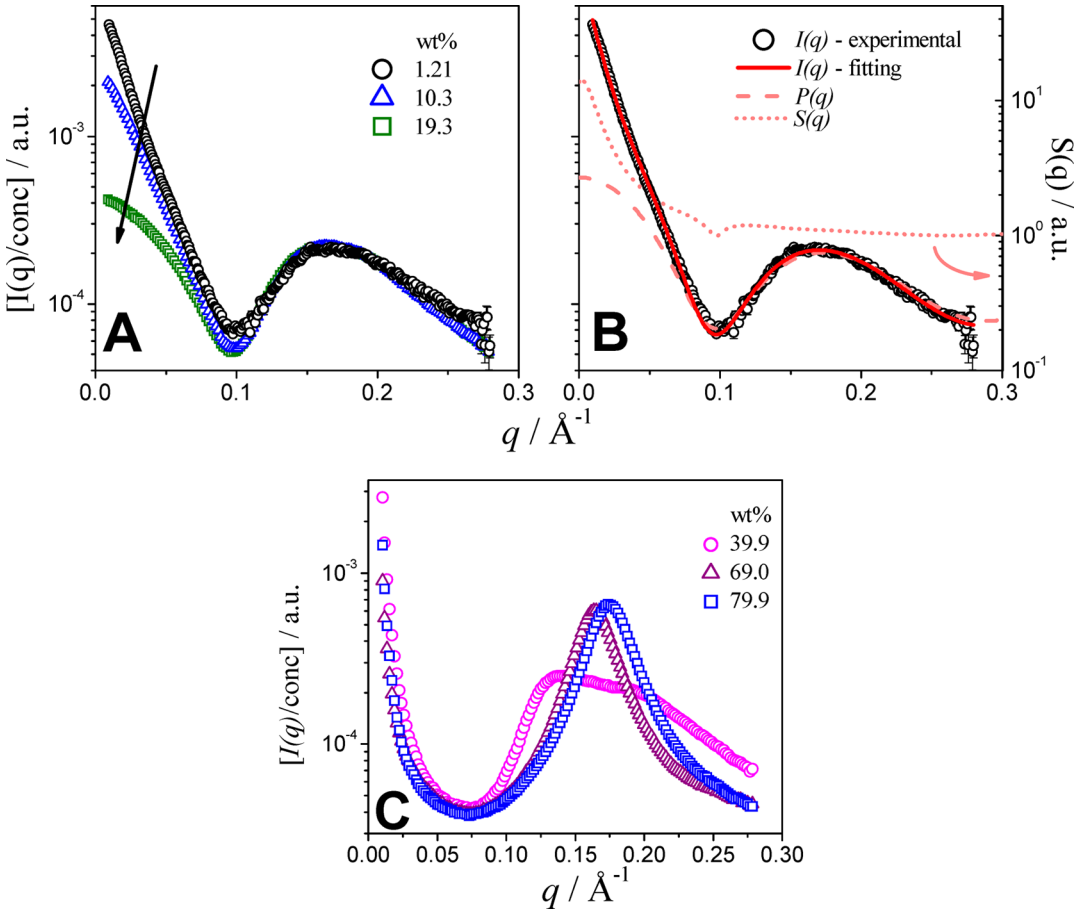

Figure 2. Concentration-normalized SAXS intensities of aqueous solutions composed of C_{16}TAP(MA-MAEO$_5$) 36:64 at different concentrations (arrow indicates the concentration increase). (A) Dilute phase. (B) Structural analysis of C_{16}TAP(MA-MAEO$_5$) 36:64 at 1.21 wt % evidencing the presence of a core−shell ellipsoidal scattering particle ($P(q)$, dashed line) and the $S(q)$ function represented by the pearl-necklace model (dotted line). The product of these two functions generates the solid line, according to eq 1. (C) Isotropic gel phase.

particles and n is the number density of scattering particles. As one can see in Figure 2A, the concentration-normalized scattering intensity of the samples at concentrations up to 20 wt % is quite similar in the $q > 0.1$ Å^{-1} region. This is an indication that the inner structural features of the scattering particles are similar among them. In the small q region ($q < 0.1$ Å^{-1}), however, there is a decrease of the normalized scattering intensity (Figure 2A), as the concentration increases (see the arrow in Figure 2A). Such an effect is related to the interaggregate correlation function that depresses the SAXS curves in the low q range as the number of aggregates increases in the system. From attempts to fit data to several $P(q)$ models (Figures S2 and S3 , see Supporting Information), it was interesting to find out that even for the most dilute system, i.e., the sample composed of C_{16}TAP(MA-MAEO$_5$) 36:64 at 1.21 wt %, it was necessary to take into account an $S(q)$ function to reproduce the corresponding SAXS curve.

For the form factor, $P(q)$, the scattering objects were modeled as an effective core−shell ellipsoid illustrated in Scheme 1. The fitting parameters were the following: R_{par}, the shortest semiaxis or inner hydrophonic core radius for the prolate ellipsoid; ν, the anisometry, which corresponds to the ratio between the longest and the shortest semiaxis; and σ, the outer hydrophilic shell thickness. For the fitting procedure, the electron density of the inner hydrophobic core (ρ_{par}) as well as the aqueous solvent (ρ_w) were kept constants at 0.275 and

Scheme 1. Representation of the Combined Models Applied to Fit SAXS Curves: a Pearl Necklace Formed by Core−Shell Ellipsoidal Micelles Interconnected by Polyions

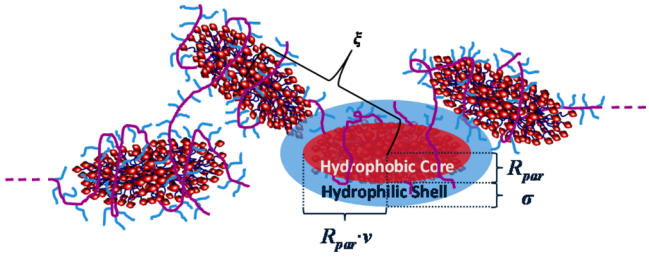

0.334 e/Å^3, respectively, whereas the electron density of the polar region was allowed to vary within the ρ_{shell} = 0.38−0.42 e/Å^3 range, according to our previous studies.[30,31]

We used the $S(q)$ function from a pearl-necklace model,[19,32,33] which has been successfully applied in the study of grafted polymers in solution.[34,35] In our case, we considered that the cationic ($C_{16}TA^+$) micelles are formed along the anionic chains of the random copolymers of P(MAA-MAEO$_5$) 36:64 and P(MAA-MAEO$_{24}$) 69:31. (Scheme 1). Of note, the pearl-necklace model was developed to describe the scattering pattern produced by a string of micelles (i.e., spherical objects with radius R, eq 2) randomly distributed along an unfolded chain[18,19,32,33] and was successfully applied to describe the

dx.doi.org/10.1021/la5019604 | Langmuir 2014, 30, 11493−11503

protein−surfactant interaction.[18] Under this methodology, $S(q)$ can be written as[18,19]

$$S(q) = 1 + \frac{1}{(qR)^{d_f}} \frac{d_f \Gamma(d_f - 1)}{(1 + (q\xi)^{-2})^{(d_f-1)/2}} \times \sin[(d_f - 1)\tan^{-1}(q\xi)] \quad (2)$$

where $\Gamma(x)$ is the gamma function, and the fractal dimension, d_f, concerns the spatial distribution of the individual scatters (the $C_{16}TA^+$-micelles) along the polymeric chain. For instance, for $d_f = 3$, the micelles are distributed in a folded polymeric chain in a compact packing, whereas $d_f < 3$ indicates that the micelles are decorating unfolded polymeric structures as represented in Scheme 1.[18,19] Furthermore, the micelle−micelle correlation has a finite range ξ, which can be seen as the characteristic distance among adjacent objects (Scheme 1). Therefore, the scattering intensity (eq 1) was modeled using the core−shell ellipsoidal micellelike aggregate for the $P(q)$ function along with the pearl-necklace model for the $S(q)$ function (eq 2). On these grounds, the effective radius R used in the $S(q)$ function (eq 2) was related to an equivalent radius of the $C_{16}TA^+$ micelles, according to the relation $R = R_{par}\nu^{1/3} + \sigma$, which assumes that the micelle and the effective sphere possess the same volume. According to such a methodology, the curves are best modeled (Figure 2) by the parameters described in Table 1.

Table 1. Fitting Parameters and Calculated Values of Volume, Number of Surfactants, and Number of Side Chains per Aggregate of Complex Salts in Water[a]

	complex salt	C_{16}TAP(MA-MAEO$_5$) 36:64	C_{16}TAP(MA-MAEO$_{24}$) 69:31
	wt %	1.21	0.48
core−shell ellipsoids	R_{par}/Å	17.9 ± 0.5	20.8 ± 0.5
	ν	1.6 ± 0.1	2.8 ± 0.2
	σ/Å	4.10 ± 0.24	7.6 ± 0.5
	R/Å	27.6 ± 0.5	37.0 ± 0.5
pearl necklace	d_f	2.15 ± 0.12	1.78 ± 0.11
	ξ/Å	100 ± 5	105 ± 5
	V_{agg}/Å^3	(3.9 ± 0.2) × 10^4	(6.8 ± 0.5) × 10^4
	N_{agg}	(8 ± 1) × 10^1	(23 ± 3) × 10^1
	N_{EOn}	(15 ± 2) × 10^1	(10 ± 1) × 10^1

[a] R_{par} is the paraffinic (hydrocarbon) radius; ν is the ratio between the largest and the smallest micelle radius; σ is the polar shell thichness; R is the effective radius of the spheres used in the pearl-necklace model; and d_f and ξ are the fractal dimension and the characteristic correlation length, respectively. V_{agg} is the volume of the micelle, and N_{agg} is the micelle aggregation number. N_{Eon} is the mean number of ethylene oxide side chains in each micelle. See the text for further details.

From the fitting parameters described in Table 1, one can evaluate the micellar core volume, V_{agg}, geometrically as $V_{agg} = (4/3)\pi R_{par}{}^3\nu$. Hence, the aggregation number, N_{agg}, can be estimated by dividing V_{agg} by the known volume of a surfactant tail with 16 carbons, according to Tanford's equation,[36] i.e., v_c = 459 Å^3. From the number ratio of $C_{16}TA^+/EO_n$ for each complex salt, the number of ethylene oxide side chains in each micelle, N_{EOn}, can also be estimated using N_{agg} (Table 1).

Furthermore, increasing the C_{16}TAP(MA-MAEO$_5$) 36:64 concentration from 19.9 to 79.9 wt % leads to the appearance of a broad correlation peak, which is also correlated with the micelle−micelle interaction (Figure 2C). Such peak appears at $q \approx 0.13$ Å^{-1} in the system composed of 39.3 wt % and shifts toward larger q values as the complex salt concentration increases. Such a shift to larger q values is related to the diminishing of the average micelle−micelle mean distance. Moreover, this effect is accompanied by a visual drastic increase in viscosity, indicating that the system is consistent with a picture of increasingly crowded aggregates. Interestingly, even under such conditions the presence of Bragg peaks was not evidenced in this system, probably owing to the great fraction of randomly distributed neutral comonomers.

3.3. C_{16}TAP(MA-MAEO$_{24}$) 69:31 + Water. Scattering curves of samples with a concentration of between 0.48 and 9.7 wt % also present a broad peak centered at $q \approx 0.14$ Å^{-1} and a well-defined minimum at $q \approx 0.06$ Å^{-1} (Figure 3). As described for the systems of C_{16}TAP(MA-MAEO$_5$) 36:64, the concentration-normalized scattering intensity shows a significant decrease at low q values as the concentration increases due to the increase in interaggregate correlation effects over the SAXS curves (Figure 3A). Hence, the same analysis used for the sample of 1.21 wt % C_{16}TAP(MA-MAEO$_5$) 36:64 was applied to the most diluted sample of C_{16}TAP(MA-MAEO$_{24}$) 69:31.

The combination of core−shell ellipsoid and pearl-necklace models was shown to be suitable to fit the scattering data for the system at 0.48 wt % (Figure 3B). All of the fitting parameters are described in Table 1.

By increasing the salt concentration in the 28 and 59 wt % range, one can notice the existence of two broad correlation peaks in the SAXS curves, with relative positions of $1^{1/2}$ and $3^{1/2}$ (Figure 3C), which gives evidence that the system is imminently forming a hexagonal mesophase. For higher concentrations, the samples are birefringent gels. In addition to these results, for the most concentrated sample investigated (with 68.4 wt % C_{16}TAP(MA-MAEO$_{24}$) 69:31), the hexagonal packing of cylinders can be identified by the Bragg reflections with relative positions of $1^{1/2}$, $3^{1/2}$, $4^{1/2}$, $7^{1/2}$, and $9^{1/2}$ related to diffraction planes 010, 110, 020, 120, and 030, respectively (Figure 3D). However, two other peaks could be associated with the same structure as diffraction planes 011 and 021. We suggest that they are related to a characteristic distance along the cylinder main axes, which could be expected if the cylinders are aggregates formed themselves by aligned micelles (Scheme 2). According to this picture, an interesting hierarchical structure is formed: each cylinder would be an aggregate formed by neighboring micelles with a characteristic repetition distance along the cylinder length. From the SAXS results for the sample with 68.4 wt % C_{16}TAP(MA-MAEO$_{24}$) 69:31 in water and using eqs S3 and S4 (Supporting Information), the unit cell parameters were calculated as a = 80.3 Å, c = 45.9 Å, and volume of unit cell $V = 2.56 \times 10^5$ Å^3.

3.4. C_{16}TAP(MA-MAEO$_5$) 72:28 + Water. The complex salt C_{16}TAP(MA-MAEO$_5$) 72:28 is not soluble in water because the system separates in two phases even at a very low concentration of complex salt (0.49 wt %). The structure of the liquid-crystalline phases was identified by SAXS, and the concentrated phase coexisting with the dilute one is a hexagonal close-packing of spheres ($P6_3/mmc$), the so-called hcp (Figure 4A). When the complex salt concentration is increased, the later phase persists and finally the structure evolves to cubic micellar ($Pm3n$) and henceforth to the hexagonal packing of cylinders ($p6mm$), as shown by SAXS in Figure 4B,C, respectively.

Table 2 presents parameters calculated for liquid-crystalline samples of C_{16}TAP(MA-MAEO$_5$) 72:28 in water using eqs

dx.doi.org/10.1021/la5019604 | Langmuir 2014, 30, 11493−11503

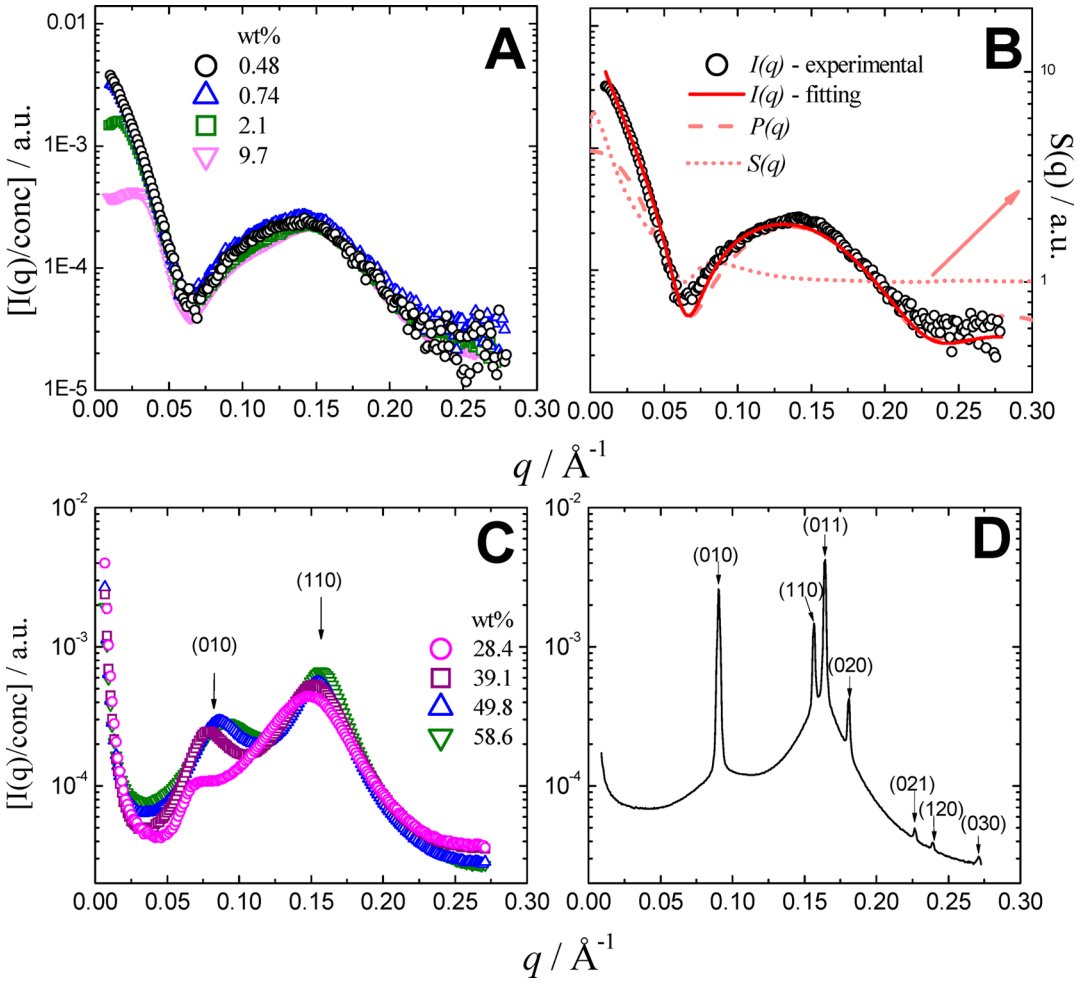

Figure 3. Concentration-normalized SAXS intensities of aqueous solutions composed of C_{16}TAP(MA-MAEO$_{24}$) 69:31 at different concentrations. (A) Dilute phase. (B) Structural analysis of C_{16}TAP(MA-MAEO$_{24}$) 69:31 at 0.48 wt % evidencing the presence of a core−shell ellipsoidal scattering particle ($P(q)$, dashed line) and the $S(q)$ function of the pearl-necklace model (dotted line). The product of these two functions generates the solid line, according to eq 1. SAXS curves of samples with different concentrations of C_{16}TAP(MA-MAEO$_{24}$) 69:31 in water forming different concentrations and forming different structures. (C) Isotropic gel phase, which is imminent in forming a hexagonal mesophase. (D) Hexagonal packing of cylindrical aggregates formed by aligned micelles (concentration of sample, 68.4 wt %). Arrows indicate the relative peak position of Bragg reflections related to the hexagonal structure. The intensity is normalized by concentration.

Scheme 2. Representation of a Hexagonal Array of Cylinders Formed by Aligned Micelles

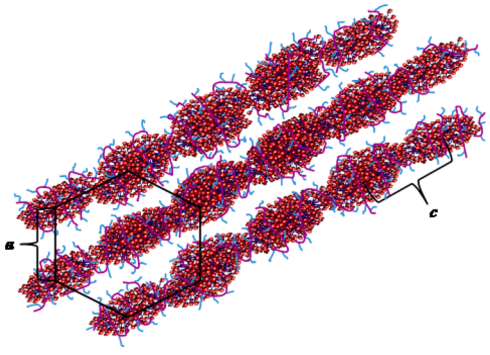

S1−S4 (Supporting Information). A single phase of the hexagonal *p6mm* structure could not be observed to allow an exact calculation of its structural parameters. However, by considering that the complex salt concentration to obtain this structure needs to be greater than 72 wt %, the minimal values of the radius of the aggregate core, r_{hc}, and the area per surfactant chain in the aggregate surface, a_s, could be estimated using eqs S5 and S6 (Supporting Information). Aggregation numbers, N_{agg}, for micelles formingliquid-crystalline phases can be estimated as described in the Supporting Information for SAXS analysis.

A remarkable characteristic of C_{16}TAP(MA-MAEO$_5$) 72:28 is the observation of an hcp structure (hexagonal close-packing of spheres with the $P6_3/mmc$ unit cell) in the concentrated phase of samples with contents of up to 54 wt % complex salt. Surfactant hcp mesophases have been reported in only a few cases, and the most well-known examples are for nonionic surfactants $C_{12}EO_8$ in water[37,38] and P123 (ethylene oxide-propylene oxide-ethylene oxide block copolymer) in mixtures of water and ethanol.[39] For complex salts of hexadecyltrimethylammonium with carboxylate-based polyions, the most commonly observed phases are the cubic packing of discrete micelles ($Pm3n$) and the hexagonal packing of cylindrical micelles ($p6mm$).[8,9,16,22,24,28] However, Chu et al. have observed a mesophase with a $P6_3/mmc$ unit cell in systems formed by the complexation of slightly cross-linked poly(sodium methacrylate-*co*-*N*-isopropylacrylamide) with tetradec-

dx.doi.org/10.1021/la5019604 | *Langmuir* 2014, 30, 11493−11503

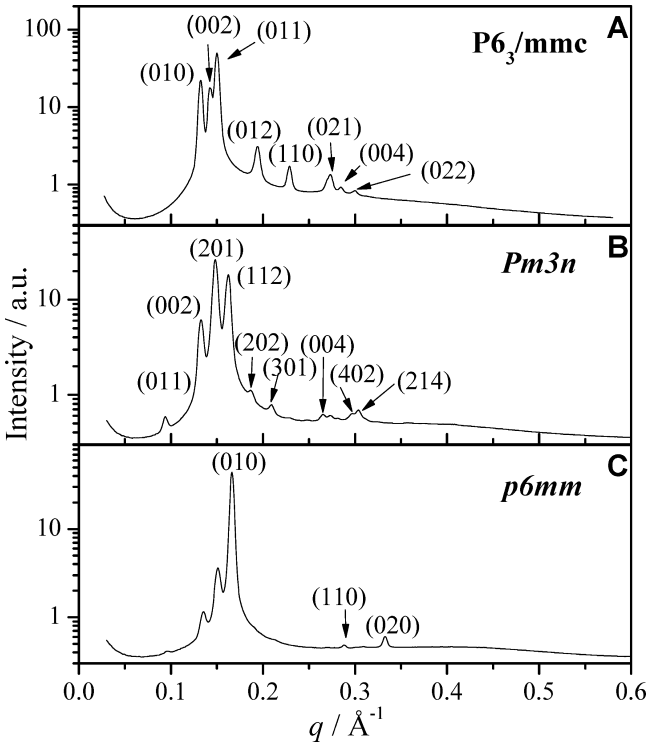

Figure 4. SAXS patterns of samples with different structures (composition of C_{16}TAP(MA-MAEO$_5$) 72:28): (A) hexagonal close-packing of spheres $P6_3/mmc$ (60 wt %), (B) cubic $Pm3n$ (66 wt %), and (C) hexagonal packing of cylinders $p6mm$ and cubic $Pm3n$ (72 wt %). Arrows indicate the relative peak positions of Bragg reflections related to the structure of major importance.

yl- or dodecyltrimethylammonium bromide in water.[40,41] The reason for the formation of hcp mesophases is still unexplored, but this structure is known to occur when the micelles are perfectly spherical and the system has dense packing. In other words, the system achieves a maximum packing fraction but minimum interfacial area between neighboring micelles. In all of the cited studies, which report the observation of hcp structure, including the present one, either a nonionic surfactant ($C_{12}EO_8$ and P123) or a copolyion with some neutral comonomers is present. It seems then that a neutral part in the headgroup is important in the formation of the hcp structure; however, it must not be the only factor.

For previously studied complex salt C_{16}TAPMA$_{80}$, it has also been observed that the first mesophase observed is $Pm3n$,[28] in contrast to the hcp for C_{16}TAP(MA-MAEO$_5$) 72:28. This means that micelles formed by C_{16}TAP(MA-MAEO$_5$) 72:28 display higher curvature than those formed by C_{16}TAPMA$_{80}$. This is probably due to the presence of neutral comonomers in the ethoxylated complex salt, which can reduce the size of the micelles, similarly to what has been reported by Norrman et al.[24] as explained above.

However, an increasing concentration of C_{16}TAP(MA-MAEO$_5$) 72:28 leads to the formation of mesophases with aggregates with lower curvature: $Pm3n$ (with slightly aspherical micelles) and $p6mm$ (with cylindrical micelles). The phase sequence indicates the unidirectional growth of the micelles, as observed for common surfactants. The slight increase in N_{agg} with increasing concentration agrees with this process (Table 2).

3.5. Structural Characterization of Water-Soluble Complex Salt Aggregate Evolution. Dilute aqueous solutions of C_{16}TAP(MA-MAEO$_{24}$) 69:31 and C_{16}TAP(MA-MAEO$_5$) 36:64 were previously investigated by dynamic light scattering.[15] On the basis of the obtained results, we proposed a model for the equilibrium aggregates. It assumed that they should be aspherical and formed by a core of surfactant micelles neutralized by polyion chains, whereas the EO side chains and neutral chain loops or tails form a hydrophilic shell (corona), which must be responsible for stabilizing the aggregates in water. Besides, we proposed that the simplest model would be a single micelle surrounded by a single polyion chain, which was consistent with the DLS data. We also considered that the polymer polydispersion could lead to the formation of aggregates with more than one micelle and/or more than one polymer chain, thus concluding that each aggregate contains at most a few polyions and a few surfactant micelles.[15]

Refined SAXS data treatment of the present study confirms the previously suggested model of aspherical aggregates with a surfactant core and a hydrophilic shell of polymer. However, existing aggregates were shown to be more complex than the proposed single-micelle/single-polyion model. After several attempts to fit SAXS data to different models, we conclude that the curves are best fitted by a model of core−shell ellipsoids to describe the form factor of each micelle combined to a pearl-necklace model (or beads on a string) to the structure factor, a model that has been previously suggested for other complexes formed by surfactants with polyelectrolytes or proteins.[18,42−45] Therefore, the combination of the two models can properly describe the whole system. It suggests that the aggregates of C_{16}TAP(MA-MAEO$_{24}$) 69:31 and C_{16}TAP(MA-MAEO$_5$) 36:64 are formed by a core of a few surfactant micelles, which are neutralized and interconnected by a few polyion chains. The ethoxylated side chains extend out from the aggregates forming the hydrophilic shell. On the basis of that, we can propose a picture of hairy pearl-necklace aggregates, as represented in Scheme 1.

The values of paraffinic radii (R_{par}) and shell thickness (σ) obtained from the SAXS data analysis (Table 1) are consistent with the values expected for a core of surfactant hydrophobic chains and a shell of oxyethylene side chains. The known calculated hydrocarbon length of the $C_{16}TA^+$ surfactant is 21.8 Å,[36] and the radius of a C_{16}TAB micelle is known to be 19.6 Å.[46] Besides, micelles in an aqueous solution of 0.1 mol L^{-1} C_{16}TAC (hexadecyltrimethylammonium chloride) were characterized by SANS as ellipsoids with a semiminor axis of 21.5 Å

Table 2. Unit Cell Characteristics, Dimensional Parameters and Aggregation Numbers for Samples of C_{16}TAP(MA-MAEO$_5$) 72:28 in Water at Different Concentrations

concentration/wt %	space group	a/Å	c/Å	V/Å^3	r_{hc}/Å	a_s/Å	N_{agg}	N_{EO5}
60	$P6_3/mmc$	54.9	89.0	2.3×10^5			84	33
66	$Pm3n$	97.2		9.2×10^5			86	33
72	$p6\ mm$	43.6			<13.1	<70.1		

dx.doi.org/10.1021/la5019604 | Langmuir 2014, 30, 11493−11503

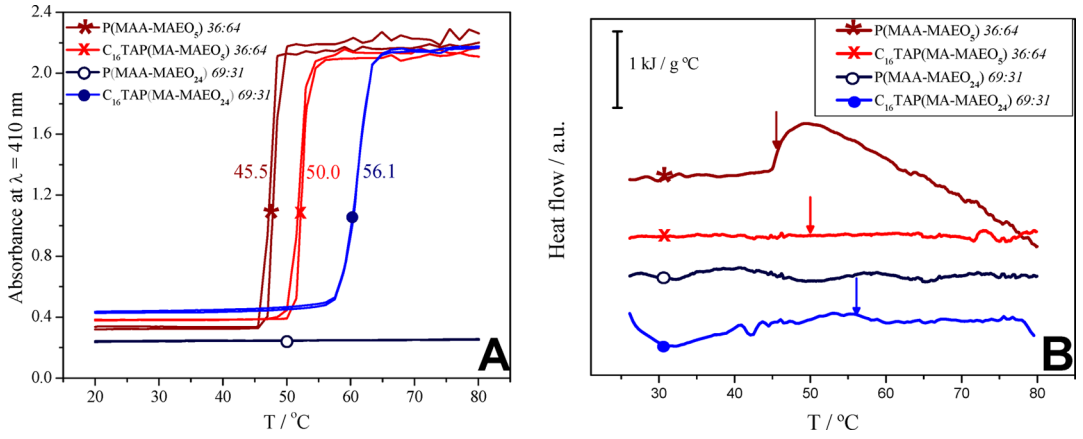

Figure 5. (A) Turbidity of solutions of polymers or complex salts (with concentrations of between 0.4 and 0.6 wt %) as a function of temperature and the respective cloud points obtained by differentiating the curves. (B) HSDSC curves of the same samples. Arrows indicate cloud-point temperatures determined by spectrophotometry. P(MAA-MAEO$_{24}$) 69:31 does not exhibit a cloud point in the studied temperature range.

and a semimajor axis of 34.7 Å.[47] For samples of C_{16}TAP(MA-MAEO$_{24}$) 69:31, which has longer side chains, the value of the shell thickness is greater than for samples of C_{16}TAP(MA-MAEO$_5$) 36:64.

DLS results from the previous study provide a diffusion coefficient of 2.5×10^{-11} m^{2}s^{-1} at infinite dilution for aqueous solutions of both C_{16}TAP(MA-MAEO$_5$) 36:64 and C_{16}TAP-(MA-MAEO$_{24}$) 69:31.[15] Assuming the pearl-necklaces aggregates to be a short cylinder, we can use eq 3 to estimate the number of micelles comprising each aggregate.

$$D = \frac{kT}{3\pi L\eta_0}\left(\ln\left(\frac{L}{d}\right) + 0.312 + \frac{0.565}{\left(\frac{L}{d}\right)} - \frac{0.1}{\left(\frac{L}{d}\right)^2}\right) \quad (3)$$

This expression is valid only in a regime where $5 < L/d < 30$, with D being the diffusion coefficient, L being the cylinder length, d being the cylinder diameter, and η_0 being the water viscosity. Assuming that d is close to $2(R_{par} + \sigma)$, we can estimate the number of micelles per aggregate to be $n = L/\xi$. From the parameters in Table 1 and using $D = 2.5 \times 10^{-11}$ m^2 s^{-1} in eq 3, we estimate that the aggregates of C_{16}TAP(MA-MAEO$_5$) 36:64 and C_{16}TAP(MA-MAEO$_{24}$) 69:31 have approximately six and five micelles, respectively.

The model suggested for the aggregates could also explain the hierarchical structure formed by mixtures of 68.4 wt % C_{16}TAP(MA-MAEO$_{24}$) 69:31 in water: the micelles interconnected by the polyions form cylinder-like aggregates that are packed into a hexagonal structure at higher concentrations. With increasing concentration, the micelles do not grow (forming, for example, elongated or worm-like micelles), but they interconnect to other micelles only by polyions, forming cylindrical aggregates. And at very high concentrations, the most favorable array for those aggregates is the hexagonal structure, as represented by Scheme 2. We speculate that it happens because of the presence of the neutral comonomers. Norrman et al. observed an increase in the curvature of aggregates for $C_{16}TA^+$ complex salts when replacing acrylate groups of the polyion chain by neutral groups, such as acrylic acid, dimethylacrylamide, or *N*-isopropylamide.[24] Similar to the authors of the mentioned article, we suggest that the presence of neutral comonomers increases the difficulty of collecting enough charged groups into a small space to neutralize micelles and that the system overcomes this situation by forming only small micelles.[24]

Taking into account the possible structures formed by the water-soluble C_{16}TAP(MA-MAEO$_n$) *x*:*y*, the polymer architecture is proven to be an important aspect affecting the structure of aggregates when comparing these results with previous studies and finding differences about the type and structure of formed aggregates. For example, in systems composed of ionic surfactant and diblock copolymers consisting of an oppositely charged block and a neutral hydrophilic block,[10−14,48] at electroneutrality, the large aggregates must be formed by a hydrophobic core that is a concentrated phase of complex salt formed by many micelles neutralized by the charged blocks. The neutral blocks form a hydrophilic shell stabilizing the dispersion in water. Owing to that, these large aggregates display dimensions, in general, of hundreds of nanometers. They are not thermodynamically stable and form structures that depend on the preparation method.[49] In addition, previous studies on complex salts of ionic surfactants and randomly grafted copolymers (with an oppositely charged backbone and neutral side chains) suggested a simpler picture for aggregates formed in aqueous solution: a hydrophobic micellar core neutralized by the polyion and stabilized by a shell of neutral hydrophilic side chains. However, the mentioned systems were not free of simple salts, and either the phase behavior or properties related to the thermodynamic stability of the system were not explored or discussed in more detail.[27,50−52]

3.6. Thermosensitivity (Nature of the Transition at the Cloud Point). Visual observation of solutions at different temperatures showed that aqueous solutions of C_{16}TAP(MA-MAEO$_5$) 36:64 and C_{16}TAP(MA-MAEO$_{24}$) 69:31 remain clear when cooled to 3 °C but become turbid when heated to higher temperatures (from 50 °C), indicating the LCST (lower critical solution temperature) behavior of the water-soluble complex salts. However, the complex salt with a lower weight fraction of ethylene oxide groups, C_{16}TAP(MA-MAEO$_5$) 72:28 (wt % of EO = 17%, Table S1, Supporting Information), phase separates in water even at very low concentration (<0.5 wt %) at room temperature, as usually observed for complex salts of homopolymers.[22,28]

The thermosensitivity of P(MAA-MAEO$_n$) *x*:*y* and C_{16}TAP-(MA-MAEO$_n$) *x*:*y* complex salts must be related to the dehydration of ethylene oxide groups upon solution heating.

dx.doi.org/10.1021/la5019604 | *Langmuir* 2014, 30, 11493−11503

The cloud points of aqueous solutions of complex salts C_{16}TAP(MA-MAEO$_5$) 36:64 and C_{16}TAP(MA-MAEO$_{24}$) 69:31, which do not form liquid-crystalline phases in dilute aqueous solutions at 25 °C, were obtained from absorbance measurements as a function of temperature as the onset of the curves. For comparison, the same procedure was performed for the respective copolymers, as shown in Figure 5A. Copolymer P(MAA-MAEO$_{24}$) 69:31 does not phase separate in the studied range of temperature, indicating that the cloud point is above 80 °C.

A similar observation and interpretation have been reported for the complex of poly(ethylene oxide)-*b*-poly(sodium methacrylate) with hexadecyltrimethylammonium bromide,[53] and for the complex of poly(sodium acrylate-*co*-sodium 2-acrylamido-2-methylpropanesulfonate)-*g*-poly(*N*-isopropylacrylamide) with dodecyltrimethylammonium bromide.[52] However, the authors of these previous studies do not characterize or discuss the structures formed in the concentrated phase after temperature-induced phase separation.

For C_{16}TAP(MA-MAEO$_5$) 36:64, which has a lower fraction of $C_{16}TA^+$ than C_{16}TAP(MA-MAEO$_{24}$) 69:31, the presence of surfactant increases the cloud point in 4.5 °C in comparison to the related acid copolymer. On the other hand, for C_{16}TAP-(MA-MAEO$_{24}$) 69:31, the cloud point is greatly decreased in the presence of $C_{16}TA^+$, probably because of a great increase in hydrophobicity. Because C_{16}TAP(MA-MAEO$_5$) 36:64 has shorter side chains than C_{16}TAP(MA-MAEO$_{24}$) 69:31, for similar contents of ethylene oxide groups, the former has a larger number of methyl terminal groups and neutral methacrylate comonomers. We suggest that because of the higher content of those hydrophobic groups, C_{16}TAP(MA-MAEO$_5$) 36:64 tends to phase separate at a lower temperature than C_{16}TAP(MA-MAEO$_{24}$) 69:31. The same argument has been used to explain why solutions of copolymers of P(MAA-MAEO$_n$) *x*:*y* with shorter side chains display lower cloud points than copolymers with the same mass fraction of ethylene oxide groups but longer side chains.[54]

In an attempt to characterize the structures formed by the complex salts in aqueous solutions at temperatures above the cloud point, some samples were chosen to be analyzed by SAXS under this condition. The chosen temperature was 70 °C, but the samples were also analyzed at 10 °C to verify the possible existence of a general trend with temperature. One could expect that at temperatures above the cloud point the aggregates concentrate to form a phase, dispersed in water, with the same structure as the phase formed at 25 °C at a high concentration of complex salt, for example, a liquid-crystalline phase formed in mixtures of C_{16}TAP(MA-MAEO$_{24}$) 69:31 in concentrations higher than 64 wt %. However, SAXS patterns of samples at 70 °C do not present the Bragg peaks expected for a liquid-crystalline phase and are different from the patterns observed for the concentrated samples at 25 °C. Moreover, the results present similar patterns for all temperatures, except that the curve is slightly shifted to longer *q* values for samples at 70 °C. (A representative example is presented in Figure S4, see Supporting Information). Hence, the turbidity is probably driven by the dehydration of EO groups and an increase in the attraction between the EO side chains of adjacent micelles, destabilizing the original micelles in water and causing them to coacervate. The result of this coacervation should be the formation of a dispersed isotropic phase that is an aqueous concentrated solution of complex salt aggregates, as observed by Mitchell et al. for dilute solutions of ethoxylated surfactants.[55]

To identify the type of phase transitions observed upon heating solutions of complex salts and the related copolymers, the same solutions used in the absorption measurements were analyzed by high-sensitivity DSC measurements. These results are summarized in Figure 5B. The thermograms do not exhibit well-defined peaks, suggesting the occurrence of transitions in which the composition of the two phases changes continuously. Only the curve of the solution of P(MAA-MAEO$_5$) 36:64 exhibits a broad peak corresponding to a low-cooperativity transition related to the cloud point. Similar behavior was previously reported for the cloud-point transition of solutions of different nonionic copolymers with ethylene oxide (EO) and propylene oxide (PO) units.[56] The absence of well-defined transition peaks confirms that the clouding process is not the formation of liquid-crystalline phases, in good agreement with the results observed by SAXS, but resembles the formation of segregated systems such as those formed by poly(ethylene oxide) in salt solutions.

4. CONCLUSIONS

We have here described the self-assembly of three distinct EO-grafted complex salts in water at different concentrations and temperatures. The SAXS technique has been demonstrated to be an invaluable tool for characterizing the assemblies and understanding the phase behavior of the complex salts. A comprehensive analysis of the binary phase diagrams of C_{16}TAP(MA-MAEO$_n$) *x*:*y* in water along with the phase diagrams of a complex salt formed by homopolyion (C_{16}TAPMA$_{80}$) reveals the effect of using grafted copolyanions on the phase behavior of complex salts. The presence of hydrophilic, ethoxylated, neutral side chains favors the formation of micelles with high curvature and tends to improve the solubility of complex salts in water. However, a minimal weight fraction of EO groups in the molecular structure has been found to be required to hinder the phase separation of complex salts in water.

The formation of water-soluble aggregates was important in characterizing the structure of dilute systems of complex salts. This is the first study involving SAXS to completely characterize aggregates of stoichiometric complex salts in dilute solutions free of simple counterions. SAXS analyses in the present study demonstrate that each formed aggregate is composed of a few surfactant micelles surrounded, interconnected, and neutralized by polyion chains with ethoxylated side chains forming an outer hydrophilic shell. There is an indication that, at higher concentrations, these aggregates are aligned in a hexagonal structure, providing an interesting example of hierarchical aggregation.

Apart from that, the structure of the concentrated phase formed by the complex salt that is not water-soluble, C_{16}TAP(MA-MAEO$_5$) 72:28, is relevant to be mentioned: the particular $P6_3/mmc$ unit cell has been identified. Furthermore, an increasing complex salt concentration leads to the unidirectional growth of the aggregates, and the structure evolves to cubic *Pm*3*n* and, eventually, hexagonal *p6mm*.

The presence of oligo(oxyethylene) chains in the complex salt structures imparts temperature sensitivity to their aqueous solutions. At their cloud temperatures, the samples become turbid in a fully reversible process.

For the above-mentioned reasons, variations in the polymer chemical structure can undoubtedly provide a rich set of

dx.doi.org/10.1021/la5019604 | *Langmuir* 2014, 30, 11493−11503

distinct structures. By changing the side-chain length, we can tailor the number of neutral comonomers, the weight fraction of EO groups, the concentration of complex salts, and structural characteristics such as the shape, aggregation number, dimensions, and packing density of micelles and aggregates. As a consequence, system properties such as solubility, the capacity to incorporate water (and perhaps a third component), the phase, and rheological behavior can be tuned. To conclude, this study has proven that the properties of systems of complex salts can be tuned by changes in the polyion structure, amplifying their potential applications. In particular, the water solubility expands the application of complex salts to aqueous systems. As a consequence, investigations of other variables of these systems are promising for the future or, as an alternative, may provide information about the effect of adding an organic solvent and the study of ternary systems.

■ ASSOCIATED CONTENT

Supporting Information

A detailed description of the materials and methods for the synthesis and characterization of copolymers, preparation of complex salts, phase diagram determination, studied mesophase composition and structure, and SAXS data analysis. This material is available free of charge via the Internet at http://pubs.acs.org.

■ AUTHOR INFORMATION

Corresponding Author

*E-mail: wloh@iqm.unicamp.br. Phone: +55 19 3521 3148. Fax: +55 19 3521 3023.

Notes

The authors declare no competing financial interest.

■ ACKNOWLEDGMENTS

We thank Professors Lennart Piculell and Karin Schillén from Lund University for valuable discussions and Brazilian agencies FAPESP and CNPq for financial support through a research grant and Ph.D. scholarship to A.M.P. and senior researcher grants to W.L., R.I., and L.R.S.B. We are also indebted to Professors Paolo Mariani and Francesco Spinozzi for providing the GENFIT software.

■ REFERENCES

(1) Thalberg, K.; Lindman, B.; Bergfeldt, K. Phase Behavior of Systems of Polyacrylate and Cationic Surfactants. *Langmuir* **1991**, *7*, 2893−2898.

(2) Piculell, L.; Lindman, B. Association and Segregation in Aqueous Polymer/Polymer, Polymer/Surfactant, and Surfactant/Surfactant Mixtures: Similarities and Differences. *Adv. Colloid Interface Sci.* **1992**, *41*, 149−178.

(3) Leung, P. S. S.; Goddard, E. D. Gels from Dilute Polymer/Surfactant Solutions. *Langmuir* **1991**, *7*, 608−609.

(4) Bronich, T. K.; Nehls, A.; Eisenberg, A.; Kabanov, V. A.; Kabanov, A. V. Novel Drug Delivery Systems Based on the Complexes of Block Ionomers and Surfactants of Opposite Charge. *Colloids Surf., B* **1999**, *16*, 243−251.

(5) Hössel, P.; Dieing, R.; Nörenberg, R.; Pfau, A.; Sander, R. Conditioning Polymers in Today's Shampoo Formulations - Efficacy, Mechanism and Test Methods. *Int. J. Cosmet. Sci.* **2000**, *22*, 1−10.

(6) Dias, R.; Melnikov, S.; Lindman, B.; Miguel, M. G. DNA Phase Behavior in the Presence of Oppositely Charged Surfactants. *Langmuir* **2000**, *16*, 9577−9583.

(7) Ganeva, D.; Antonietti, M.; Faul, C. F. J.; Sanderson, R. Polymerization of the Organized Phases of Polyelectrolyte-Surfactant Complexes. *Langmuir* **2003**, *19*, 6561−6565.

(8) Piculell, L.; Svensson, A.; Norrman, J.; Bernardes, J. S.; Karlsson, L.; Loh, W. Controlling Structure in Associating Polymer-Surfactant Mixtures. *Pure Appl. Chem.* **2007**, *79*, 1419−1434.

(9) Piculell, L.; Norrman, J.; Svensson, A. V. A. V.; Lynch, I.; Bernardes, J. S.; Loh, W. Ionic Surfactants with Polymeric Counterions. *Adv. Colloid Interface Sci.* **2008**, *147−148*, 228−236.

(10) Bronich, T. K.; Kabanov, A. V.; Kabanov, V. A.; Yu, K.; Eisenberg, A. Soluble Complexes from Poly(ethylene Oxide)-Block-Polymethacrylate Anions and N-Alkylpyridinium Cations. *Macromolecules* **1997**, *30*, 3519−3525.

(11) Bronich, T. K.; Popov, A. M.; Eisenberg, A.; Kabanov, V. Af.; Kabanov, A. V. Effects of Block Length and Structure of Surfactant on Self-Assembly and Solution Behavior of Block Ionomer Complexes. *Langmuir* **2000**, *16*, 481−489.

(12) Pispas, S. Complexes of Polyelectrolyte-Neutral Double Hydrophilic Block Copolymers with Oppositely Charged Surfactant and Polyelectrolyte. *J. Phys. Chem. B* **2007**, *111*, 8351−8359.

(13) Berret, J.-F.; Oberdisse, J. Electrostatic Self-Assembly in Polyelectrolyte-Neutral Block Copolymers and Oppositely Charged Surfactant Solutions. *Phys. B* **2004**, *B 350*, 204−206.

(14) Berret, J.-F.; Vigolo, B.; Eng, R.; Hervé, P.; Grillo, I.; Yang, L. Electrostatic Self-Assembly of Oppositely Charged Copolymers and Surfactants: A Light, Neutron, and X-ray Scattering Study. *Macromolecules* **2004**, *37*, 4922−4930.

(15) Percebom, A. M.; Janiak, J.; Schillén, K.; Piculell, L.; Loh, W. Micellization of Water-Soluble Complex Salts of an Ionic Surfactant with Hairy Polymeric Counterions. *Soft Matter* **2013**, *9*, 515−526.

(16) Svensson, A.; Piculell, L.; Cabane, B.; Ilekti, P. A New Approach to the Phase Behavior of Oppositely Charged Polymers and Surfactants. *J. Phys. Chem. B* **2002**, *106*, 1013−1018.

(17) Hammersley, A. *FIT2D: An Introduction and Overview*; European Synchrotron Radiation Facility Internal Report, 1997.

(18) Santos, S. F. S.; Zanette, D.; Fischer, H.; Itri, R. A Systematic Study of Bovine Serum Albumin (BSA) and Sodium Dodecyl Sulfate (SDS) Interactions by Surface Tension and Small Angle X-ray Scattering. *J. Colloid Interface Sci.* **2003**, *262*, 400−408.

(19) Teixeira, J. Small-Angle Scattering by Fractal Systems. *J. Appl. Crystallogr.* **1988**, *21*, 781−785.

(20) Percebom, A. M.; Piculell, L.; Loh, W. Polyion-Surfactant Ion Complex Salts Formed by a Random Anionic Copolyacid at Different Molar Ratios of Cationic Surfactant. Phase Behavior with Water and N-Alcohols. *J. Phys. Chem. B* **2012**, *116*, 2376−2384.

(21) Svensson, A.; Piculell, L.; Karlsson, L.; Cabane, B.; Jönsson, B. Phase Behavior of an Ionic Surfactant with Mixed Monovalent/Polymeric Counterions. *J. Phys. Chem. B* **2003**, *107*, 8119−8130.

(22) Svensson, A.; Norrman, J.; Piculell, L. Phase Behavior of Polyion- Surfactant Ion Complex Salts: Effects of Surfactant Chain Length and Polyion Length. *J. Phys. Chem. B* **2006**, *110*, 10332−10340.

(23) Norrman, J.; Piculell, L. Phase Behavior of Cetyltrimethylammonium Surfactants with Oligo Carboxylate Counterions Mixed with Water and Decanol: Attraction between Charged Planes or Spheres with Oligomeric Counterions. *J. Phys. Chem. B* **2007**, *111*, 13364−13370.

(24) Norrman, J.; Lynch, I.; Piculell, L. Phase Behavior of Aqueous Polyion-Surfactant Ion Complex Salts: Effects of Polyion Charge Density. *J. Phys. Chem. B* **2007**, *111*, 8402−8410.

(25) Leal, C.; Bilalov, A.; Lindman, B. The Effect of Postadded Ethylene Glycol Surfactants on DNA-Cationic Surfactant/Water Mesophases. *J. Phys. Chem. B* **2009**, *113*, 9909−9914.

(26) Janiak, J.; Piculell, L.; Olofsson, G.; Schillén, K. The Aqueous Phase Behavior of Polyion-Surfactant Ion Complex Salts Mixed with Nonionic Surfactants. *Phys. Chem. Chem. Phys.* **2011**, *13*, 3126−3138.

(27) Nisha, C. K.; Basak, P.; Manorama, S. V.; Maiti, S.; Jayachandran, K. N. Water-Soluble Complexes from Random Copolymer and Oppositely Charged Surfactant. 1. Complexes of

Poly(ethylene Glycol)-Based Cationic Random Copolymer and Sodium Dodecyl Sulfate. *Langmuir* **2003**, *19*, 2947−2955.
(28) Bernardes, J. S.; Loh, W. Structure and Phase Equilibria of Mixtures of the Complex Salt Hexadecyltrimethylammonium Polymethacrylate, Water and Different Oils. *J. Colloid Interface Sci.* **2008**, *318*, 411−420.
(29) Bendedouch, D.; Chen, S.-H. Study of Intermicellar Interaction and Structure by Small Angle Neutron Scattering. *J. Phys. Chem.* **1983**, *87*, 1653−1658.
(30) Barbosa, L. R. S.; Caetano, W.; Itri, R.; Homem-de-Mello, P.; Santiago, P. S.; Tabak, M. Interaction of Phenothiazine Compounds with Zwitterionic Lysophosphatidylcholine Micelles: Small Angle X-Ray Scattering, Electronic Absorption Spectroscopy, and Theoretical Calculations. *J. Phys. Chem. B* **2006**, *110*, 13086−13093.
(31) Santiago, P. S.; Neto, D.; de, S.; Barbosa, L. R. S.; Itri, R.; Tabak, M. Interaction of Meso-Tetrakis (4-Sulfonatophenyl) Porphyrin with Cationic CTAC Micelles Investigated by Small Angle X-ray Scattering (SAXS) and Electron Paramagnetic Resonance (EPR). *J. Colloid Interface Sci.* **2007**, *316*, 730−740.
(32) Chen, S.-H.; Teixeira, J. Structure and Fractal Dimension of Protein-Detergent Complexes. *Phys. Rev. Lett.* **1986**, *57*, 2583−2586.
(33) Guo, X. H.; Zhao, N. M.; Chen, S. H.; Teixeira, J. Small-Angle Neutron Scattering Study of the Structure of Protein/Detergent Complexes. *Biopolymers* **1990**, *29*, 335−346.
(34) Berts, I.; Gerelli, Y.; Hilborn, J.; Rennie, A. R. Structure of Polymer and Particle Aggregates in Hydrogel Composites. *J. Polym. Sci., Part B: Polym. Phys.* **2013**, *51*, 421−429.
(35) D'Errico, G.; De Lellis, M.; Mangiapia, G.; Tedeschi, A.; Ortona, O.; Fusco, S.; Borzacchiello, A.; Ambrosio, L. Structural and Mechanical Properties of UV-Photo-Cross-Linked poly(N-Vinyl-2-Pyrrolidone) Hydrogels. *Biomacromolecules* **2008**, *9*, 231−240.
(36) Tanford, C. *The Hydrophobic Effect: Formation of Micelles and Biological Membranes*; Wiley: New York, 1973; p 52.
(37) Ospinal-Jiménez, M.; Pozzo, D. C. Structural Analysis of Protein Complexes with Sodium Alkyl Sulfates by Small-Angle Scattering and Polyacrylamide Gel Electrophoresis. *Langmuir* **2011**, *27*, 928.
(38) Hassan, N.; Barbosa, L. R. S.; Itri, R.; Ruso, J. M. Fibrinogen Stability under Surfactant Interaction. *J. Colloid Interface Sci.* **2011**, *362*, 118−126.
(39) Holmberg, K.; Jönsson, B.; Kronberg, B.; Lindman, B. *Surfactants and Polymers in Aqueous Solution*, 2nd ed.; John Wiley & Sons, Ltd: Chichester, U.K., 2002; p 281.
(40) Thalberg, K.; Lindman, B.; Karlström, G. Phase Behavior of a System of Cationic Surfactant and Anionic Polyelectrolyte: The Effect of Salt. *J. Phys. Chem.* **1991**, *95*, 6004−6011.
(41) Swanson-Vethamuthu, M.; Almgren, M.; Karlsson, G.; Bahadur, P. Effect of Sodium Chloride and Varied Alkyl Chain Length on Aqueous Cationic Surfactant-Bile Salt Systems. Cryo-TEM and Fluorescence Quenching Studies. *Langmuir* **1996**, *12*, 2173−2185.
(42) Aswal, V. K.; Goyal, P. S. Counterions in the Growth of Ionic Micelles in Aqueous Electrolyte Solutions: A Small-Angle Neutron Scattering Study. *Phys. Rev. E: Stat., Nonlinear, Soft Matter Phys.* **2000**, *61*, 2947−2953.
(43) Vitorazi, L.; Berret, J.-F.; Loh, W. Self-Assembly of Complex Salts of Cationic Surfactants and Anionic-Neutral Block Copolymers. Dispersions with Liquid-Crystalline Internal Structure. *Langmuir* **2013**, *29*, 14024−14033.
(44) Berret, J.-F.; Cristobal, G.; Hervé, P.; Oberdisse, J.; Grillo, I. Structure of Colloidal Complexes Obtained From Neutral/Polyelectrolyte Copolymers and Oppositely Charged Surfactants. *Eur. Phys. J. E: Soft Matter Biol. Phys.* **2002**, *9*, 301−311.
(45) Nisha, C. K.; Manorama, S. V.; Jayachandran, K. N.; Maiti, S. Water-Soluble Complexes from Random Copolymer and Oppositely Charged Surfactant. 2. Complexes of Poly(ethylene Glycol)-Based Cationic Random Copolymer and Bile Salts. *Langmuir* **2004**, *20*, 8468−8475.
(46) Balomenou, I.; Bokias, G. Water-Soluble Complexes between Cationic Surfactants and Comb-Type Copolymers Consisting of an Anionic Backbone and Hydrophilic Nonionic poly(N, N-Dimethylacrylamide) Side Chains. *Langmuir* **2005**, *21*, 9038−9043.
(47) Tsolakis, P.; Bokias, G. Temperature-Sensitive Water-Soluble Polyelectrolyte/Surfactant Complexes Formed between Dodecyltrimethylammonium Bromide and a Comb-Type Copolymer Consisting of an Anionic Backbone and Poly(N-Isopropylacrylamide) Side Chains. *Macromolecules* **2006**, *39*, 393−398.
(48) Clerck, M. A New Symmetry for the Packing of Amphiphilic Direct Micelles. *J. Phys. II* **1996**, *6*, 961−968.
(49) Imai, M.; Yoshida, I.; Iwaki, T.; Nakaya, K. Static and Dynamic Structures of Spherical Nonionic Surfactant Micelles during the Disorder-Order Transition. *J. Chem. Phys.* **2005**, *122*, 1−9.
(50) Soni, S. S.; Brotons, G.; Bellour, M.; Narayanan, T.; Gibaud, A. Quantitative SAXS Analysis of the P123/water/ethanol Ternary Phase Diagram. *J. Phys. Chem. B* **2006**, *110*, 15157−15165.
(51) Zhou, S.; Burger, C.; Yeh, F.; Chu, B. Charge Density Effect of Polyelectrolyte Chains on the Nanostructures of Polyelectrolyte−Surfactant Complexes. *Macromolecules* **1998**, *31*, 8157−8163.
(52) Zhou, S.; Yeh, F.; Burger, C.; Chu, B. Formation and Transition of Highly Ordered Structures of Polyelectrolyte-Surfactant Complexes. *J. Phys. Chem. B* **1999**, *103*, 2107−2112.
(53) Solomatin, S. V.; Bronich, T. K.; Eisenberg, A.; Kabanov, V. A.; Kabanov, A. V. Colloidal Stability of Aqueous Dispersions of Block Ionomer Complexes: Effects of Temperature and Salt. *Langmuir* **2004**, *20*, 2066−2068.
(54) Jones, J. A.; Novo, N.; Flagler, K.; Pagnucco, C. D.; Carew, S.; Cheong, C.; Kong, X. Z.; Burke, N. A. D.; Stöver, H. D. H. Thermoresponsive Copolymers of Methacrylic Acid and Poly (ethylene Glycol) Methyl Ether Methacrylate. *J. Polym. Sci., Part A: Polym. Chem.* **2005**, *43*, 6095−6104.
(55) Mitchell, D. J.; Tiddy, G. J. T.; Waring, L.; Bostock, T.; McDonald, M. P. Phase Behaviour of Polyoxyethylene Surfactants with Water: Mesophase Structures and Partial Miscibility (Cloud Points). *J. Chem. Soc., Faraday Trans. 1* **1983**, *79*, 975−1000.
(56) Niemiec, A.; Loh, W. Interaction of Ethylene Oxide-Propylene Oxide Copolymers with Ionic Surfactants Studied by Calorimetry: Random versus Block Copolymers. *J. Phys. Chem. B* **2008**, *112*, 727−733.